Hybrid k-preemptive Transmission Scheme for Minimal Age of Information in IoT Networks

Badiaa Gabr, Ahmed H. Sakr, Hesham ElSawy, Karim G. Seddik, and Wessam Mesbah

***Abstract*—This paper explores the Age of Information (AoI) in IoT networks, aiming to minimize the average AoI for real-time applications. We employ a spatiotemporal model with a heterogeneous Poisson field (HPF) of interferers and an absorbing Markov chain (AMC) to quantify AoI dynamics. This model specifically examines the effects of packet segmentation (i.e., rate adaptation) to maintain a stable rate in the presence of IoT interference. Unlike previous works focused on preemptive and non-preemptive schemes, we propose a novel hybrid k-preemptive transmission scheme. This scheme dynamically decides whether to continue or preempt transmission based on the number of delivered segments, addressing interference issues. Simulation results demonstrate the superiority of the proposed scheme over conventional schemes, consistently minimizing the average AoI.**

***keywords*—** Age of Information (AoI), Stochastic Geometry, Preemptive and Non-preemptive Queue.

I. Introduction

The Internet of Things (IoT) is a rapidly growing technology reshaping industries through enhanced efficiency, cost reduction, and enriched user experiences. Since many IoT applications operating in real-time with minimal delay tolerance, ensuring timely data reception is paramount. Therefore, AoI has been adopted as a performance metric to quantify data freshness [1]. AoI tracks the time elapsed since the generation of the most recent successfully delivered packet at the receiver. AoI is usually studied via queueing theory to track the time elapsed from packet generation to transmission under different traffic generation patterns and packet scheduling schemes. In large-scale and dense networks, stochastic geometry is jointly utilized with queueing theory to account for the network interference impact on AoI [2], [3]. This approach allows us to capture the statistical insights necessary to understand the behavior of large-scale networks and optimize long-term system-level parameters in environments where device connectivity and density fluctuate. The integration between stochastic geometry and queuing theory is well-known in the literature as spatiotemporal analysis, which is thoroughly presented in [4].

Spatiotemporal analysis is utilized in [5] to study the AoI for random and duty-cycled packet generation, however, under non-preemptive packet scheduling only. Preemptive and non-preemptive packet scheduling are compared in [6], however, for small sized packets that do not need fragmentation. For large-sized packets, rate adaptation via packet fragmentation is studied in [7] to minimize delay, which does not necessarily minimize AoI. The impact of packet segmentation on AoI is studied in [8], however, for the conventional non-preemptive and preemptive transmission schemes.

This paper introduces a novel k-preemptive transmission scheme that minimizes AoI in large-scale IoT networks, where the preemption decision depends on the number of already delivered segments of the same packet. Assuming that different IoT devices are distributed as a heterogeneous Poisson point process (PPP) and utilizing an absorbing Markov chain (AMC) to track segments transmissions, we develop a novel spatiotemporal that characterizes and benchmarks the proposed k-preemptive transmission scheme. Our numerical results show that the hybrid k-preemptive transmission scheme consistently outperforms both conventional schemes when the preemption level k is designed carefully.

II. System Model

This work focuses on a scenario involving an arbitrary IoT transmitter-receiver pair sharing spectrum with other IoT devices. The intended IoT pair is separated by a distance D_0. Interfering IoT devices are spatially distributed according to a static PPP Ψ in $\mathbb{R}^2$ with intensity λ. To account for the diversity among coexisting IoT devices, the interference at the intended link is modeled via a heterogeneous Poisson field (HPF). The HPF consists of V different network types that differ in their transmission powers w_v and activity factors A_v, where $v \in \{1, 2, \ldots, V\}$. The type of each IoT device is independent of its spatial location, and hence, Ψ can be divided into V independent PPPs, denoted hereafter as Ψ_v with intensities $\lambda_v = f_v(v)\lambda$, where $f_v(v)$ is the probability of belonging to type v. Transmissions are subject to power-law path loss and Rayleigh fading, where $h \sim \mathcal{CN}(0, 1)$ is the normalized baseband channel gain and $d^{-\eta}$ is the power decay model with the distance d and path-loss exponent $\eta > 2$. Note that channel state information is unknown at the transmitter.

We assume a time-slotted system with independent block channel fading across different time slots. The fixed realization of the HPF is justified by the slow rate of change in network

B. Gabr is with the Department of Electronic Engineering, Maynooth University, W23 F2H6, Ireland (email: badiaa.gabr.2025@mumail.ie). A. H. Sakr is with the Department of Electrical and Computer Engineering, University of Windsor, Windsor, ON, N9B 3P4 Canada, (email: ahmed.sakr@uwindsor.ca). H. ElSawy is with the School of Computing, Queen's University, Kingston, ON, K7L 3N9 Canada, (email: hesham.elsawy@queesu.ca). K.-G. Seddik is with the Electronics and Communications Engineering Department, American University in Cairo, New Cairo 11835, Egypt, (email: kseddik@aucegypt.edu). W. Mesbah is with the Electrical Engineering Department, and Center for Communication Systems and Sensing, King Fahd University of Petroleum & Minerals (KFUPM), Dhahran 31261, KSA, (email: mesbahw@kfupm.edu.sa).

The authors would like to acknowledge the support provided by the Deanship of Research Oversight and Coordination (DROC) at King Fahd University of Petroleum & Minerals (KFUPM) for funding under the Interdisciplinary Research Center for Communication Systems and Sensing through project No. INCS2201.

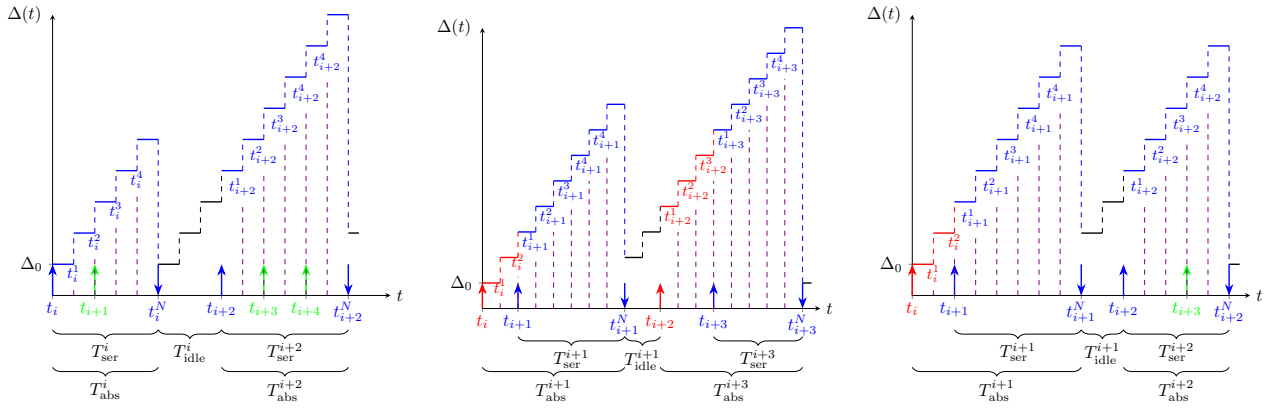

(a) Non-preemptive scheme (b) Preemptive scheme (c) k-preemptive scheme

Fig. 1: Evolution of AoI for the non-preemptive, preemptive, and k-preemptive schemes for a segmentation policy of $N = 5$ segments per packet. Upwards and downwards blue arrows represent in-service packet generations and successful packet transmissions, respectively. Green arrows and red arrows represent dropped packets and interrupted packets, respectively.

geometry compared to the short time slot duration. Consequently, the intended IoT device experiences interference from IoT devices at fixed but random locations, experiencing varying activities and channel fading gains across different time slots. To accommodate the random HPF realization, we consider C performance classes based on the transmission success probability (TSP). Using stochastic geometry analysis in Section V, the likelihood of the intended IoT device belonging to one of these classes is derived from the meta distribution of the TSP.

The intended IoT transmitter operates with a one-packet size queue, randomly generating data packets (e.g., sensor updates) with probability a per time slot. Each packet has a size of $\mathcal{L}$ bits, which can be further segmented into N smaller segments for reliable transmission at a rate determined by the channel condition. The transmission rate $\mathcal{R}_N$ is calculated as

$$\mathcal{R}_N = \frac{\mathcal{L}}{N \times T_s} = \zeta W \log_2(1 + \theta_N), \tag{1}$$

where W denotes the channel bandwidth, T_s is the time slot duration, ζ captures the gap to the theoretical Shannon's capacity, and θ_N is the minimum signal-to-interference-ratio (SIR) threshold required to successfully decode a segment at the intended receiver. All segments have to be successfully received at the receiver to reconstruct and decode the packet. An AMC is employed to track the transmission progress of segments within the same packet, with absorption indicating successful packet completion.

III. Hybrid k-preemptive Transmission Scheme

This section discusses two common preemption schemes in the literature: non-preemptive and preemptive schemes. Then, it introduces the concept of k-preemptive transmission that blends elements of both non-preemptive and preemptive schemes, allowing for a degree of flexibility in task scheduling.

1) Non-preemptive Transmission Scheme: In this scheme, once a packet transmission begins, the sender is committed to completing the transmission of all segments. If new packets are generated while some segments are still in service, these packets are discarded. Fig. 1(a) tracks the evolution of AoI of the non-preemptive scheme starting from the arrival of an arbitrary packet at time t_k. The successful delivery of the k^{th} segment of the i^{th} packet is highlighted by the dashed line labeled t_i^k. It can be seen that new packets that are generated during the service of the current packet are dropped (e.g., $i+1$, $i+3$, and $i+4$). After successful delivery of the in-service packets (e.g., at t_i^N and t_{i+2}^N), the transmitter becomes idle until the generation of a new packet (e.g., at t_{i+2}).

2) Preemptive Transmission Scheme: In this scheme, a newly generated packet interrupts the transmission of the current in-service packet to ensure the transmission of the most up-to-date information. Nevertheless, this does not always guarantee minimum AoI due to wasting partial delivery of in-service packets. It can be seen in Fig. 1(b) that the new packets (e.g., $i+1$ and $i+3$) interrupt all pending segments in the in-service packets (e.g., i and $i+2$, respectively), and transmission of 5 new segments is started.

3) k-preemptive Transmission Schemes: Neither the preemptive nor the non-preemptive scheme guarantees achieving the minimum AoI. The preemptive scheme prioritizes delivering the most updated information, but this comes at the cost of discarding partially transmitted packets, resulting in wastage. On the other hand, the non-preemptive scheme avoids wasting partial packet transmissions but does so at the expense of discarding fresh information. Here, we propose a hybrid scheme that aims to strike a balance between these approaches to minimize AoI. To achieve this balance and ensure both information freshness and efficient transmission, we introduce a preemption level parameter $0 \leq k \leq N$, which influences the preemptive behavior of the system. That is, the transmitter initially operates in preemptive mode, then after successfully delivering k segments of a packet, it switches to non-preemptive mode. Hence, smaller values of k lead to less frequent preemptions, while larger values indicate more aggressive preemption. Note that when $k = 0$, the hybrid

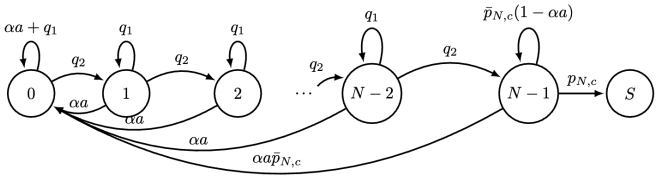

Fig. 2: Unified DTMC for the packet transmission with N segments.

scheme is equivalent to the non-preemptive scheme and when $k = N$, it is equivalent to the preemptive scheme.

For a pictorial illustration, we demonstrate a 3-preemptive scheme in Fig. 1(c). The transmitter initially operates in preemptive mode at t_i. Upon receiving a new packet at t_{i+1}, the transmission of Packet i is interrupted since only two segments (i.e., less than k segments) have been delivered at that time. The transmitter then resumes preemptive mode after successfully delivering Packet $i+1$ at time t^N_{i+1}. Subsequently, the transmitter begins transmitting Packet $i+2$ at time t_{i+2}. After successfully delivering $k = 3$ segments of Packet $i+2$, it switches to non-preemptive mode at time t^3_{i+2}. Hence, newly generated packets (e.g., at t_{i+3}) are dropped and the transmitter is committed to the completion of the remaining segments of Packet $i+2$ initiated at t_{i+2}.

In Fig. 1, the inter-arrival idle time is denoted as T_{idle}. The time to absorption T_{abs} is derived from an AMC constructed in Section IV to track the duration from the generation of the first packet after a successful reception to the completion of service. On the other hand, service time T_{ser} refers to the duration taken to successfully deliver all segments that belong to the same packet. It is important to note that tasks are not interrupted once initiated in the non-preemptive scheme, hence $T_{\text{abs}} = T_{\text{ser}}$. Conversely, in the preemptive scheme, interruptions are possible, leading to potential differences such that $T_{\text{abs}} \geq T_{\text{ser}}$, particularly if the current packet is interrupted. In the k-preemptive scheme, the time to absorption may or may not differ from the service time, depending on which segment of the packet is interrupted.

IV. Temporal Age of Information (AoI) Analysis

The performance of the intended IoT link depends on the employed segmentation policy along with the spatial realization of the surrounding HPF of interferers. Let the tuple (N, c) denote the adopted number of segments and the success probability class for the intended link. We then construct a discrete-time AMC (DT-AMC) for each (N, c) pair. The categorization of the classes and the success probability $p_{N,c}$ within each class are described in Section V.

The adopted DT-AMC tracks the successful delivery of segments where packets can be generated at any instant inside the time slot and the absorption state indicates that all segments are successfully delivered. For the sake of generalized analysis, let $\alpha \in \{0, 1\}$ be the preemption factor defined as $\alpha = \mathbb{1}_{\{n \leq k\}}$, where $\mathbb{1}_{\{\cdot\}}$ is the indicator function. In the k-preemptive transmission scheme, the preemption level k controls the transition from preemption to non-preemption scheme at the $(k+1)^{th}$ segment, thereby preventing the loss of successful delivery of the previous k segments. The adopted definition of α enables a unified construction of the DT-AMC shown in Fig. 2 with a transition matrix $T_{N,c} =$

$$\left[\begin{array}{c:c} Q_{N,c} & H_{N,c} \\ \hdashline 0 & 1 \end{array}\right] = \left[\begin{array}{ccccc:c} \alpha a + q_1 & q_2 & 0 & \cdots & 0 & 0 \\ \alpha a & q_1 & q_2 & \cdots & 0 & 0 \\ \alpha a & 0 & q_1 & \cdots & 0 & 0 \\ \vdots & 0 & \ddots & \ddots & \vdots & \vdots \\ \alpha a \bar{p}_{N,c} & 0 & \cdots & 0 & q_1 & p_{N,c} \\ \hdashline 0 & 0 & 0 & 0 & 0 & 1 \end{array}\right], \tag{2}$$

where $\bar{(\cdot)} = 1 - (\cdot)$ denotes the complement probability, $q_1 = \bar{p}_{N,c}(1 - \alpha a)$ accounts for failed segment delivery and $q_2 = p_{N,c}(1 - \alpha a)$ accounts for successful segment delivery. In (2), the $N \times N$ sub-stochastic matrix $Q_{N,c}$ tracks the transmissions of the N segments that belong to the in-service packet and $H_{N,c}$ is an $N \times 1$ vector that tracks the transition of the absorbing state, which implies the successful delivery of the last segment. In the preemptive scheme, the incoming packet replaces older segments, causing the DT-AMC to restart and wasting the transmission of older segments. This is shown in (2) and Fig. 2 via the factor αa that restarts the DT-AMC to its initial state of transmitting the first segment. In this context, the instantaneous AoI $\Delta(t)$ is defined as the time elapsed since the generation of the last successfully delivered packet. As shown in Fig. 1, starting from an initial AoI $\Delta(0) \doteq \Delta_0$, the discretized AoI at the receiver increases with time in a staircase fashion and drops upon the reception of a new packet.

For a given segmentation policy, the AoI calculation depends on the average time to absorption T_{abs}, the average service time T_{ser}, and the inter-arrival idle time T_{idle}. A consistent definition of T_{abs} for all schemes will be the time taken from the end of an idle state due to a new packet generation to the beginning of the next idle state due to successful packet delivery at a rate $\mathcal{R}_N$. Following the DT-AMC analysis in [9, Section 3.6], the average numbers of time slots to absorption can be obtained as $M_{\text{abs}} = \beta(I - Q_{N,c})^{-1}\mathbf{1}$, where β is the initial state vector, I is the $N \times N$ identity matrix, and $\mathbf{1}$ is an $N \times 1$ vector of 1's. Since we always start from the first segment, upon packet arrival, the $1 \times N$ initialization vector is $\beta = [1, 0, 0, \cdots, 0]$. Given the time slot duration T_s, the average time to absorption is $T_{\text{abs}} = T_s M_{\text{abs}}$.

Let M^i_{ser} denote the number of time slots required to deliver all N segments of packet i. Then, $T^i_{\text{ser}} = T_s M^i_{\text{ser}} = t^N_i - t_i$. In the k-preemptive scheme, M^i_{ser} is the sum of two independent non-identical negative binomial random variables; $M^i_{\text{ser,p}}$ during the preemptive period and $M^i_{\text{ser,n}}$ for the non-preemptive period. It is straightforward to show that the distributions of both random variables are expressed as:

$$\begin{aligned} \mathbb{P}\{M^i_{\text{ser,p}} = m_p\} &= \binom{m_p - 1}{k - 1} p^k_{N,c}(1 - p_{N,c})^{m_p - k}(\bar{a})^{m_p - 1}, \\ \mathbb{P}\{M^i_{\text{ser,n}} = m_n\} &= \binom{m_n - 1}{N - k - 1} p^{N-k}_{N,c}(1 - p_{N,c})^{m_n - N + k}, \end{aligned} \tag{3}$$

where $m_p \geq k$ and $m_n \geq N - k$. Note that in the non-preemptive scheme with $k = 0$, the service time is the same

as the time to absorption, as illustrated in Fig. 1. Using the distribution in (3), the average service time of a packet $T_{\text{ser}} = \mathbb{E}(M^i_{\text{ser,n}}) + \mathbb{E}(M^i_{\text{ser,p}})$ is calculated as $\mathbb{E}(M^i_{\text{ser,n}}) = \frac{N-k}{p_{N,c}}$ and

$$\mathbb{E}(M^i_{\text{ser,p}}) = \frac{\sum_{m_p=k}^{\infty} m_p \mathbb{P}\{M^i_{\text{ser,p}} = m_p\}}{\sum_{m_p=k}^{\infty} \mathbb{P}\{M^i_{\text{ser,p}} = m_p\}}. \tag{4}$$

Furthermore, the inter-arrival time $T^i_{\text{idle}} = T_s M^i_{\text{idle}}$ measures the time between the successful delivery of Packet i at the receiver and the generation of the next packet at the transmitter. By virtue of the memoryless property of Markovian models, the distribution of M^i_{idle} is geometric with probability mass function $\mathbb{P}(M^i_{\text{idle}} = m_i) = a(1-a)^{m_i-1}$, from which we can calculate the average as $T_{\text{idle}} = \frac{T_s}{a}$. Given T_{abs}, T_{ser}, and T_{idle}, the average AoI can be calculated as:

$$\text{AoI} = \mathbb{E}(\Delta(t)) = T_{\text{ser}} + \frac{1}{2}(T_{\text{abs}} + T_{\text{idle}}). \tag{5}$$

V. Spatial SIR Analysis

This section derives the transmission success probability (TSP) $p_{N,c}$, where the class c depends on the realization of the HPF Ψ around the intended IoT link. For segmentation policy N and an arbitrary realization of the HPF Ψ, the TSP at the intended receiver can be expressed as

$$p_N = \mathbb{P}\left(\frac{w_t h_0 D_0^{-\eta}}{\sum_{v=1}^{V} \sum_{u \in \Psi_v} \mathbb{1}_{\{A_v\}} w_v h_u D_u^{-\eta}} > \theta_N | \Psi \right), \tag{6}$$

where w_t represents the transmission power, D_0 and h_0 are the link length and channel gain of the intended IoT link, D_u and h_u are the link length and channel gain from the u-th interfering IoT device to the intended receiver, and $\mathbb{1}_{\{A_v\}}$ is the indicator function that accounts for the activities of the devices. Averaging over fading gains and devices activities [7], [10], the TSP for segmentation policy N is given by

$$p_N = \prod_{v=1}^{V} \prod_{D_u \in \Psi_v} \left(\frac{A_v}{1 + \theta_N \frac{w_v D_0^{\eta}}{w_t D_u^{\eta}}} + (1 - A_v) \right). \tag{7}$$

As there is no prior information regarding the exact configuration of the interfering IoT network Ψ, we employ the meta distribution to assess the probability of the target link operating at a particular success probability [10]. Following [7], [10], we adopt the beta distribution to approximate the meta-distribution; $\bar{F}(\theta_N, \gamma) = \mathbb{P}\{p_N > \gamma)\}$, as follows:

$$\bar{F}(\theta_N, \gamma) = 1 - \mathcal{I}_{\gamma}\left(\frac{\mu_N(\mu_N - \nu_N)}{\nu_N - \mu_N^2}, \frac{(1-\mu_N)(\mu_N - \nu_N)}{\nu_N - \mu_N^2} \right), \tag{8}$$

where $\mathcal{I}_{\gamma}(a, b)$ is the regularized incomplete beta function, μ_N and ν_N are the first and second moments of p_N across different realizations of the HPF Ψ, and are given by [7]:

$$\mu_N = \exp\left(-\Lambda \theta_N^{\frac{2}{\eta}} \sum_{v=1}^{V} \left(\frac{w_v}{w_t} \right)^{\frac{2}{\eta}} k_v \lambda_v \right), \tag{9}$$

$$\nu_N = \exp\left(-\Lambda \theta_N^{\frac{2}{\eta}} \sum_{v=1}^{V} \left(\frac{w_v}{w_t} \right)^{\frac{2}{\eta}} k_v \lambda_v \left(2 - \left(1 - \frac{2}{\eta} \right) k_v \right) \right), \tag{10}$$

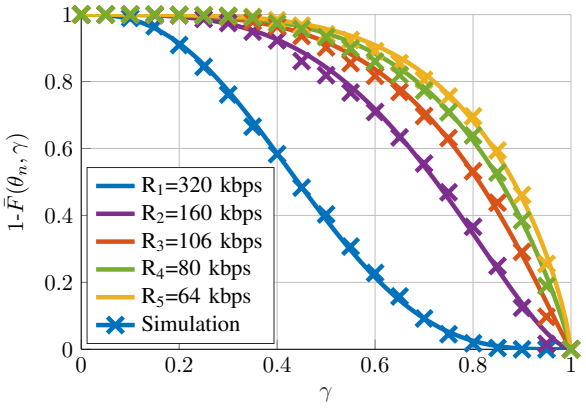

Fig. 3: TSP meta-distribution for different values of $\mathcal{R}_N$ with packet size $L = 40$ Bytes and $N \in \{1, 2, 3, 4, 5\}$ segments.

where $\Lambda = \frac{2(\pi D_0)^2}{\eta \sin(2\pi/\eta)}$. $\bar{F}(\theta_N, \gamma)$ reflects the percentage of HPF realizations where the target link is expected to operate with TSP p_N exceeding γ. To obtain meaningful per-class TSP $p_{N,c}$, we discretize (8) into C equiprobable classes. Let $\zeta_0 = 0$ and $\zeta_C = 1$, and choose $\{\zeta_1, \zeta_2, \cdots, \zeta_{C-1}\}$ that satisfy $\bar{F}(\theta_N, \zeta_i) - \bar{F}(\theta_N, \zeta_{i-1}) = \frac{1}{C}$, for all $i = 1, 2, \cdots, C-1$. Then, $p_{N,c}$ for each class is the median value within the boundaries $[\zeta_c, \zeta_{c+1}]$, which can be obtained through

$$\bar{F}(\theta_N, \zeta_c) - \bar{F}(\theta_N, p_{N,c}) = \frac{1}{2C}. \tag{11}$$

VI. Numerical Results

Following [7], [11], we validate the analysis via Monte Carlo simulations over an area of 4.5 km^2 with 1,000 different HPF realizations over 10,000 time iterations. Unless stated otherwise, the parameters for HPF are set as follows: $\lambda = 0.001$ devices/m^2, divided into $V = 3$ different networks with a uniform distribution $f_v(v) = 1/3$ where $v \in \{1, 2, 3\}$, and transmit power and activity factors $w_v \in \{10, 7, 5\}$ mW and $k_v \in \{0.1, 0.3, 0.5\}$, respectively. An arrival rate of $a = 0.1$ is considered along with the following link parameters: $W = 100$ kHz, $\zeta = 0.8$, $\eta = 4$, $D_0 = 20$ meters, and $N = 5$ rates. To find $p_{N,c}$, the meta-distribution in (8) is evaluated for $C = 35$ equiprobable TSP classes for different HPF realizations. Fig. 3 presents $\bar{F}(\theta_N, \gamma)$ for different transmission rates and confirms that both the analysis and simulation results of each TSP meta-distribution are identical.

In the following, we compare the AoI of the proposed hybrid k-preemptive scheme with different preemption levels, ranging from non-preemptive to preemptive, as discussed in Section II. Several parameters affect the AoI, including packet arrival rate, channel quality, packet size, and number of segments. However, due to space limitation, we combine the effects of channel quality and packet size into one parameter; the success probability. In each figure, we maintain a constant arrival rate a and a number of segments N, facilitating comparative analysis of different schemes across varying success probabilities.

In Fig. 4(a), we examine the scenario with $a = 0.1$ and $N = 3$, showcasing the AoI of all possible preemption levels (i.e., $k = 0, 1, 2$, and 3) across different success probability classes.

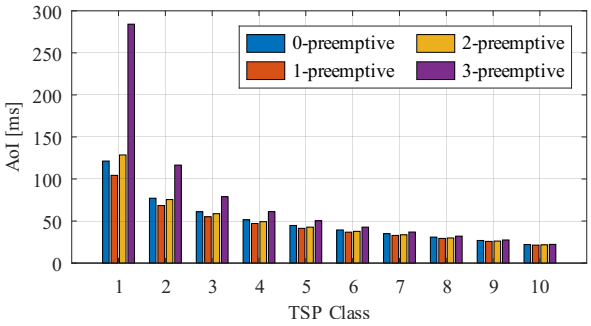

(a) $N = 3$ segments/packet (i.e., $\mathcal{R}$=213.3 kbps)

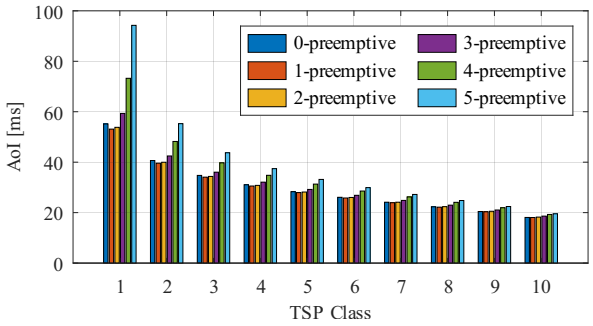

(b) $N = 5$ segments/packet (i.e., $\mathcal{R}$=128 kbps)

Fig. 4: Average AoI with arrival rate $a = 0.1$ and packet size $L = 80$ Bytes for $C = 10$ TSP classes.

Note that 0-preemptive and 3-preemptive refer to the non-preemptive and preemptive schemes, respectively. Notably, increasing the success probability substantially reduces the AoI across all schemes. Under conditions of poor channel quality (i.e., low success probabilities), the 1-preemptive scheme outperforms all other schemes, including the non-preemptive scheme, as it prioritizes completing ongoing transmissions over initiating new ones, particularly when success probabilities are low. This behavior holds across various success probabilities, although the advantage diminishes as success probability increases. Conversely, the preemptive scheme (i.e., the 3-preemptive scheme) exhibits the highest AoI due to its tendency to prematurely terminate ongoing transmissions in favor of new arrivals. These findings underscore the importance of adaptively selecting transmission mode based on prevailing channel conditions and arrival rates.

Fig. 4(b) replicates the experiment for $N = 5$ and confirms the findings observed in Fig. 4(a). It indicates that there exists a preemption level k beyond which switching to a non-preemptive strategy increases the average AoI. Fig. 4 also underscores the benefits of segmentation, wherein increasing the number of segments from $N = 3$ to $N = 5$ leads to a reduction in AoI. This reduction occurs because, for a given packet size and time slot duration, a higher number of segments results in smaller segment sizes that can be transmitted at a lower rate with a relaxed SIR threshold, hence, improving the success probability. The improved success probability results in fewer retransmissions, leading to a shorter time to absorption and service time (i.e., lower AoI). However, there exists an optimal N beyond which the AoI increases, due to the increase in the number of segments required to be successfully received, which corroborates the findings of [7].

Overall, the results highlight the benefits of the proposed hybrid k-preemptive scheme and the importance of rate adaptation to minimize AoI in wireless IoT networks. The work in [6] identified preemptive schemes as optimal for non-segmented packet transmission. However, our analysis considers packet segmentation, which introduces complexities that favor alternative transmission strategies. Therefore, the apparent contradiction stems from differing underlying assumptions.

VII. Conclusion

In this work, we developed a spatiotemporal model to analyze the AoI of a target IoT link within a large-scale IoT network. Our model considers IoT devices distributed according to a heterogeneous Poisson field of interferers, and we investigated the average AoI using an absorbing Markov chain framework. Additionally, we incorporated packet segmentation and proposed a novel hybrid k-preemptive scheme. Our study evaluated the average AoI of conventional non-preemptive and preemptive schemes, as well as the k-preemptive scheme, across various system parameters. Our numerical results highlight the superiority of the k-preemptive scheme that preempts packet transmission only if fewer than k segments are delivered. This scheme consistently outperforms both conventional schemes when an appropriate preemption level is selected.

References

[1] S. K. Kaul, R. D. Yates, and M. Gruteser, "Real-time status: How often should one update?" *2012 Proceedings IEEE INFOCOM*, pp. 2731–2735, 2012.

[2] G. Chisci, H. Elsawy, A. Conti, M.-S. Alouini, and M. Z. Win, "Uncoordinated massive wireless networks: Spatiotemporal models and multiaccess strategies," *IEEE/ACM Transactions on Networking*, vol. 27, no. 3, pp. 918–931, 2019.

[3] M. Song, H. H. Yang, H. Shan, J. Lee, and T. Q. S. Quek, "Age of information in wireless networks: Spatiotemporal analysis and locally adaptive power control," *IEEE Transactions on Mobile Computing*, vol. 22, no. 6, pp. 3123–3136, 2023.

[4] X. Lu, M. Salehi, M. Haenggi, E. Hossain, and H. Jiang, "Stochastic geometry analysis of spatial-temporal performance in wireless networks: A tutorial," *IEEE Commun. Surv. Tutor.*, vol. 23, pp. 2753–2801, 2021.

[5] M. Emara, H. ElSawy, and G. Bauch, "A spatiotemporal model for peak AoI in uplink IoT networks: Time versus event-triggered traffic," *IEEE Internet of Things Journal*, vol. 7, no. 8, pp. 6762–6777, 2020.

[6] P. D. Mankar, M. A. Abd-Elmagid, and H. S. Dhillon, "Spatial distribution of the mean peak age of information in wireless networks," *IEEE Trans. Wireless Commun.*, vol. 20, no. 7, pp. 4465–4479, 2021.

[7] H. ElSawy, "Rate adaptation and latency in heterogeneous IoT networks," *IEEE Commun. Lett.*, vol. 25, no. 2, pp. 660–664, 2021.

[8] B. Gabr, H. ElSawy, K. G. Seddik, and W. Mesbah, "Age of information for preemptive/non-preemptive transmissions in large-scale IoT networks," in *GLOBECOM 2022 - 2022 IEEE Global Communications Conference*, 2022, pp. 329–334.

[9] A. S. Alfa, *Applied discrete-time queues*. Springer, 2016.

[10] M. Haenggi, "The meta distribution of the SIR in Poisson bipolar and cellular networks," *IEEE Trans. Wireless Commun.*, vol. 15, no. 4, pp. 2577–2589, 2016.

[11] ——, *Stochastic Geometry for Wireless Networks*. Cambridge University Press, 2012.